AUTHOR(S): HRIDYA, S., KAVITHA, V.S., CHALANA, S.R., RESHMI KRISHNAN, R., SREEJA SREEDHARAN, R., SURESH, S., NAMPOORI, V.P.N., SANKARARAMAN, S., PRABHU, R. and MAHADEVAN PILLAI, V.P.

TITLE: Study on the structural, morphological and optical properties of RF-sputtered dysprosium-doped barium tungstate thin films.

YEAR: 2017

Publisher citation: HRIDYA, S., KAVITHA, V.S., CHALANA, S.R., RESHMI KRISHNAN, R., SREEJA SREEDHARAN, R., SURESH, S., NAMPOORI, V.P.N., SANKARARAMAN, S., PRABHU, R. and MAHADEVAN PILLAI, V.P. 2017. Study on the structural, morphological and optical properties of RF-sputtered dysprosium-doped barium tungstate thin films. JOM: journal of the Minerals, Metals and Materials Society [online], 69(11), pages 2272-2277. Available from: https://doi.org/10.1007/s11837-017-2360-4

OpenAIR citation: HRIDYA, S., KAVITHA, V.S., CHALANA, S.R., RESHMI KRISHNAN, R., SREEJA SREEDHARAN, R., SURESH, S., NAMPOORI, V.P.N., SANKARARAMAN, S., PRABHU, R. and MAHADEVAN PILLAI, V.P. 2017. Study on the structural, morphological and optical properties of RF-sputtered dysprosium-doped barium tungstate thin films. JOM: Journal of the Minerals, Metals and Materials Society, 69(11), pages 2272-2277. Held on OpenAIR [online]. Available from: https://openair.rgu.ac.uk

Study on the Structural, Morphological and Optical Properties of RF Sputtered Dysprosium Doped Barium Tungstate Thin Films

Hridya.S[1], Kavitha V.S[1], Chalana S.R[1],Reshmi Krishnan R[1], SreejaSreedharan R[1], S. Suresh[1], V.P.N.Nampoori[1], S. Sankararaman[1], Radhakrishna Prabhu[2]and V.P. MahadevanPillai[1*]

1Department of Optoelectronics, University of Kerala, Kariavattom, Thiruvananthapuram - 695581, Kerala, India.
[2]School of Engineering, Robert Gordon University, Aberdeen, UK

***Email:**vpmpillai9@gmail.com

Abstract: Barium tungstate ($BaWO_4$)films with different Dy^{3+} doping concentrations namely 0,1,3and 5wt% are deposited on cleaned quartz substrate by radio frequency (RF) magnetron sputtering technique and the prepared films are annealed at a temperature of 700 ˚C. The structural, morphological and optical properties of the annealed films are studied using techniques such as X-ray diffraction (XRD), micro-Raman spectroscopy, field emission scanning electron microscopy (FESEM), atomic force microscopy (AFM) and photoluminescence (PL) spectroscopy. XRD analysis shows that all the films are well-crystallized in nature with monoclinic barium tungstate phase. The presence of characteristic modes of tungstate group in the Raman spectra supports the formation of barium tungstatephase in the films.Scanning electron microscopic (SEM) images of the films present uniform dense distribution of well-defined grains with different sizes. All the doped films present a broad emission in the 390-500 nm region and its intensity increases up to 3 wt% and there after decreases due to usual concentration quenching.

1. Introduction

Over the past two decades ardent research has been going on for the design and synthesis of functional micro/nano materials with precise size and morphology, because the dimensional and structural characteristics of these materials offer wide range of potential applications in various fields such as optics, electronics, magnetics, and biology [1]. Tungstate is a family of inorganic materials, among them Barium tungstate ($BaWO_4$) is the heaviest and is known for its wide range of applications in lasers, radiation detection, photo luminescence etc.[2].Alkaline-earth metal tungstatesAWO_4 ($A=Ba^{2+}$, Ca^{2+} and Sr^{2+}) have high refractive index, high chemical stability and high X-ray absorption coefficient which make them suitable for optical and display technologies[3]. Metal tungstates are prepared and characterized by different techniques such as thermal evaporation [4], electron beam evaporation [5],chemical vapour deposition [6], pulsed laser deposition [7, 8] and RF magnetron sputtering[9]. Dysprosium is a suitable dopant for many inorganic lattices which produce white light emission by suitably adjusting the yellow and blue emissions [10]. In the present investigation dysprosium doped $BaWO_4$ films are prepared using RF magnetron sputtering technique and the structural, morphological and optical properties of the films annealed at a temperature of 700 ˚C are investigated using techniques such as X-ray diffraction (XRD), micro-Raman spectroscopy, field emission scanning electron microscopy (FESEM), atomic force microscopy(AFM) and photoluminescence spectroscopy(PL).

2. Experimental Details

Dysprosium doped barium tungstate thin films are deposited on cleaned quartz substrates at room temperature (300 K) using RF magnetron sputtering technique. Targets for the films are prepared from commercially available barium tungstate powder (Sigma Aldrich, purity-99.99 %) and dysprosium oxide (Sigma Aldrich, purity-99.99 %) powder. Two grams of the barium tungstate powder is weighed accurately and mixed with 0, 1, 3 and 5 wt% of dysprosium oxide powderand the mixture is then ground well in an agate motor with a pestle. The pressed powder is used as the target for the preparation of films. The sputter chamber is initially evacuated to a base pressure of 10^{-6}mbar and pure argon gas is admitted into the chamber and the argon pressure is maintained at 0.015 mbar. The target is powered through a magnetron power supply (HINDHIVAC MODEL-12 "MSPT") operated at a frequency of 13.56 MHz and the RF power of 150 W is maintained during sputtering. The distance between the target and the substrate is kept at 50 mm. The sputter time is kept constant at 30 minutes for all the samples. The films are prepared with dysprosium doping concentrations of 0, 1, 3 and 5 wt% and the prepared films are annealed at a temperature of 700 $^{\circ}$C. The films thus obtained are designated as B0, B1, B3 and B5 respectively.

The crystalline structure and crystallographic orientation of the films are characterized by X-ray diffraction measurements [BRUKER ADVANCE 8] in the 2θ range 20-80°employing Cu Kα1 radiation with a wavelength of 1.5406 Å in the 2θ range 20°-70° at a scan rate of 0.02° per minute, micro- Raman spectra of the films are recorded using Labram -HR 800 spectrometer at a spectral resolution of about 1 cm^{-1} equipped with Peltier cooled Synapse CCD detector system maintained at -70 °C and the spectra is recorded with an excitation wavelength of 514 nm from an argon ion laser. Surface morphology and compositional analysis of the thin film samples are studied using scanning electron microscope [Nova NanoSEM NPEP252, (Bruker)] measurements. Photoluminescence spectra of the films are recorded using Fluoromax-4 Spectrophotometer [HORIBA JOBIN JOHN] with an excitation radiation at wavelength 350 nm from Xenon Lamp.

3 Results and Discussion

3.1 XRD Analysis

Fig. 1(a) shows the XRD patterns of pure and dysprosium doped $BaWO_4$ films which are annealed at a temperature of700°C. All films present well-defined peaks at 2 values 26.08°, 27.54°, 30.48°,42.55°,48.24°,54.45° and 57.43° which can be indexed to lattice reflection planes(1 1),(0 2 1),(2 1),(1 2),(3 1),(2 2 2),(4 2 3) and (8 1 0) respectively of monoclinic wolframite phase of $BaWO_4$ (JCPDS 70-1048) suggesting their polycrystalline nature. In the XRD patterns of allthe films, (1 1) and (0 2 1) peaks appear as prominent peaks, with intensity shifting depending on the Dy^{3+} doping concentration. In the XRD pattern of B0 film the (0 2 1) peak appears with higher intensity compared to that of (1 1) peak. As the Dy^{3+} doping concentration increases the intensity of (1 1) peak enhances up to 3 wt% and thereafter decreases considerably with increase in Dy^{3+} doping concentration. The intensity of (0 2 1) peak shows a reduction in B1 film compared to that of B0 film and then increases in B3 film. In the B5 film the intensity of this peak is slightly less than that in the B3 film. The overall XRD intensity is the highest for the B3 film.

Also, the full width at half maximum (FWHM) calculated for the highest intense peak in the XRD patterns decreases systematically with doping concentration up to 3 wt% and thereafter increases. Thus moderate doping of dysprosium is found to enhance the crystalline quality of the films whereas higher dysprosium doping reduces the crystallinity of the films. In the undoped film the preferred orientation of crystal growth is along (0 2 1) plane. Interestingly the preferred orientation of crystal growth changes to (1 1) plane on mild doping of Dy^{3+} (up to 3wt %). At higher doping concentration (5wt %) the preferred orientation of crystal growth again changes to (0 2 1) plane. Thus, dysprosium doping in $BaWO_4$ lattice influences its crystal structure. The average size of the crystallites in the films are calculated using the Scherer formula [11] and Williamson-Hall plot [12]. The calculated values are shown in Table I. This indicates the nanostructured nature of the films.

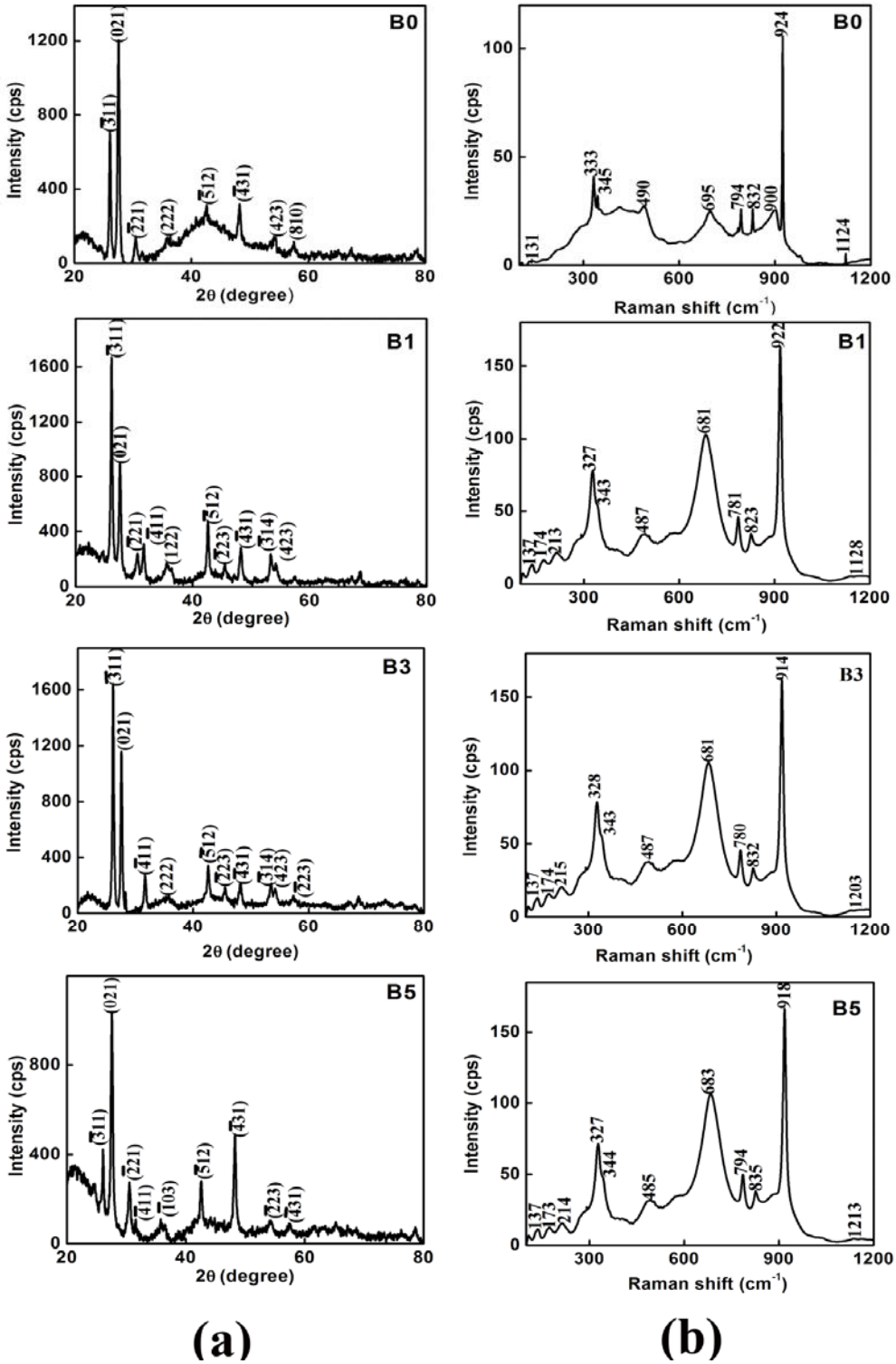

Fig. 1. (a) XRD patterns of the undoped and Dy^{3+} doped $BaWO_4$ films deposited by RF magnetron sputtering technique and post annealed at a temperature 700 ˚C and (b) Micro Raman spectra of undoped and Dy^{3+} doped $BaWO_4$ films deposited by RF magnetron sputtering technique and post annealed at a temperature of 700 ˚C.

Table I. Structural and morphological properties of undoped and Dy^{3+} doped $BaWO_4$ thin films prepared by RF magnetron sputtering and post annealed at a temperature of 700° C.

Sample code	Average size of the crystallites (nm)		rms surface roughness (nm)
	From scherrer formula	From W-H plot	
B0	22	27	4.17
B1	25	37	16.38
B3	28	49	27.68
B5	23	43	12.32

3.2 Micro-Raman analysis

Fig.1(b) shows the micro-Raman spectra of the undoped and dysprosium doped $BaWO_4$ thin films which are annealed at a temperature 700 ^{0}C. The most intense bandin the Raman spectra of the undoped film at 924 cm^{-1}can be assigned to the symmetric stretching mode of W-O bond [13]. The asymmetric stretching mode of W-O bond [13] appears with large splitting as intense bands at 695 and 900 cm^{-1} and medium intense bands at794and 832 cm^{-1}. Thus, this mode exhibits additional splitting apart from the lifting of degeneracy. The splitting observed for the asymmetric stretching mode can be an indication of the distortion of the WO_4 tetrahedra in the film [14].

In the Raman spectra of Dy^{3+}doped $BaWO_4$ films the W-O symmetric stretching mode appears at lower wave numbers compared to that observed for the undoped film. Also this mode shows an enhancement in intensity in the doped films. The full width half maximum (FWHM) of symmetric stretching mode in the undoped film is 3.03 cm^{-1} and for the doped filmsits value is much higher. The enhancement in the broadness of the symmetric stretching mode can be attributed to the enhanced strain in the doped films.The medium intense bands in the Raman spectra of the films in the wave number range 300- 490 cm^{-1} can be attributed to the bending vibrations of tungstate group. The bands below 200 cm^{-1} can be due to the lattice vibrations [14].

3.3 FESEM Analysis

The FESEM images of undoped and Dy^{3+} doped $BaWO_4$ thin films are shown in Fig. 2(a). The SEM image of the B0 film presents a uniform dense distribution of smaller grains and a random distribution of bigger clusters of different sizes. The SEM images of Dy^{3+} doped films also present a uniform dense distribution of smaller grains and a random distribution of bigger clusters. But the size of the larger clusters in the dysprosium doped films are lesser

compared to that in undoped film. The SEM images of Dy^{3+} doped films also show a tendency of the bigger clusters to form networks of large sizes.

AFM images of undoped and Dy^{3+} doped $BaWO_4$ thin films are shown in Fig. 2(b). AFM image of undoped film (B0) shows an agglomerated mode of grain growth. The AFM image of the doped films presents distribution of well-defined grains. As seen in the SEM images, the tendency of grains to form bigger structures can be seen in the AFM images of the doped films. The rms surface roughness's of the films are calculated from the AFM data and the values are shown in Table I. The B0 film shows the lowest value of rms roughness (4.17 nm) and B3 film shows the highest value of rms roughness (27.68 nm).

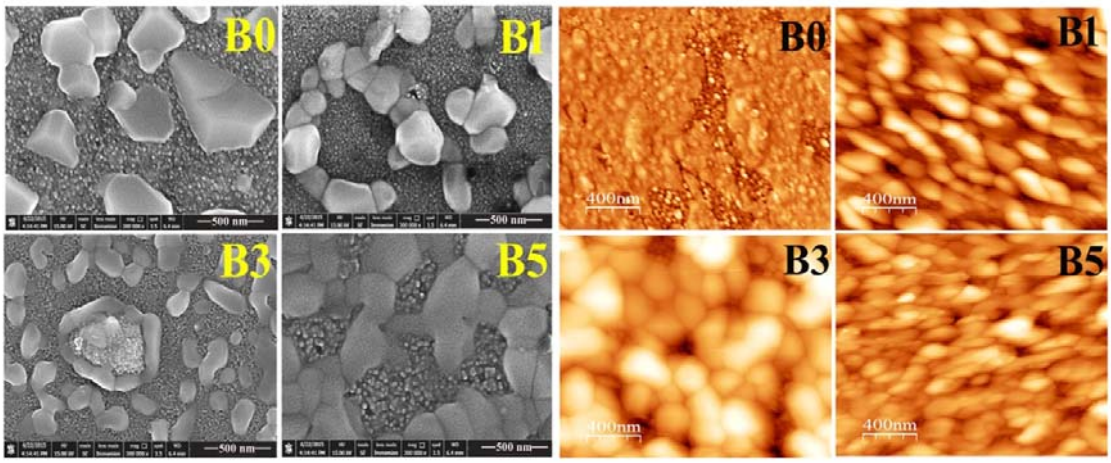

Fig. 2(a) SEM images of undoped and Dy^{3+} doped $BaWO_4$ thin films prepared by RF magnetron sputtering and post annealed at a temperature of 700° C and (b) AFM images of undoped and Dy^{3+} doped $BaWO_4$ thin films prepared by RF magnetron sputtering and post annealed at a temperature of 700° C.

3.4 Photoluminescence analysis

The photoluminescence (PL) spectra of undoped and Dy^{3+} doped $BaWO_4$ films were recorded using an excitation radiation of wavelength 350 nm [Fig. 3(a)]. Undoped $BaWO_4$ film presents no PL emission. All doped films present a broad emission ranging from 390-500 nm. As the doping percentage increases, the intensity of the PL emission increases up to 3 wt% and there after decreases due to usual concentration quenching. It is interesting to note that the intensity of the PL emission in the B5 film is the lowest among the doped films. This can be attributed to quenching of PL emission arising out of nonradiative processes like cross relaxation between neighbouring Dy^{3+} ions [15].

In the present case, pure $BaWO_4$ film does not show any band structure as in the case of doped films. Hence, we can attribute the observed spectral peaks in the Dy^{3+} doped $BaWO_4$ films to transitions corresponding to

dysprosium ions. The PL spectra of dysprosium ions in $BaWO_4$ films contains a single broad and intense band in the 460 nm region. The band shows a structure of multiple peaks. Hence, we deconvoluted the observed spectra to reveal the underlying structure. The deconvoluted PL spectra of the doped films are presented in Fig. 3(b)-(d). The deconvoluted PL spectra consists of three peaks at 412, 434 and 460 nm for all the films.

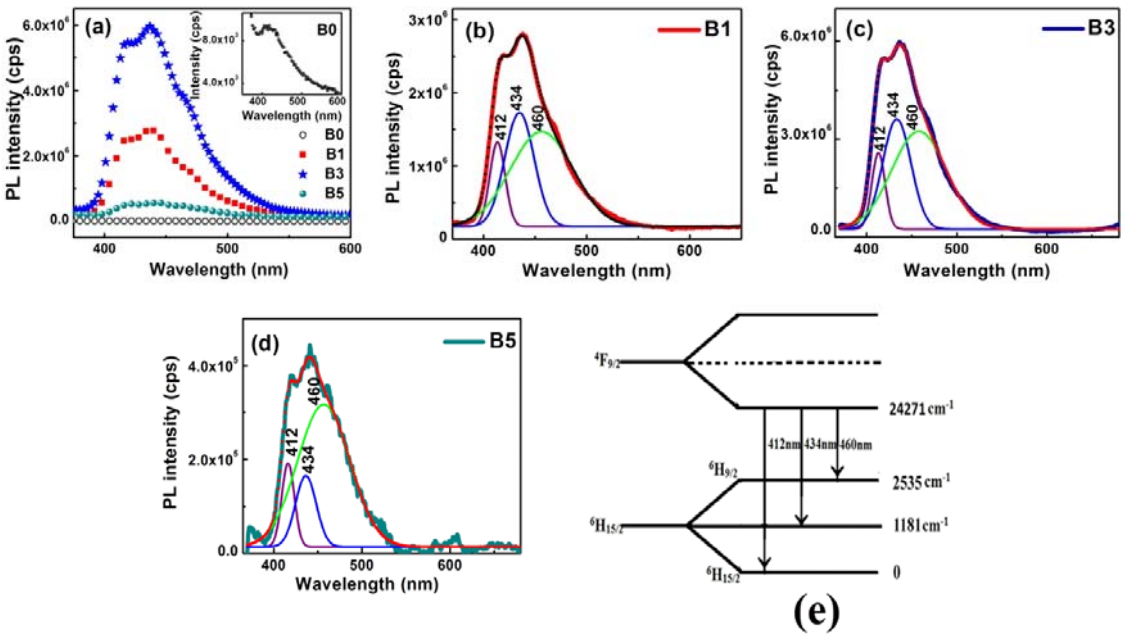

Fig. 3(a) Photoluminescence spectra of undoped and Dy^{3+}doped $BaWO_4$ films, (b)-(d) deconvoluted photoluminescence spectra of Dy^{3+}doped $BaWO_4$films showing splitting of peaks and (e) approximate energy level diagram showing $^4F_{9/2}$-$^6H_{15/2}$ transitions of Dy^{3+}ions in $BaWO_4$

Xiaoyu et al., observed PL emissions at 489 and 570 nm in Dy^{3+} doped $BaWO_4$ powder and reported these blue and yellow emissions due to f–f transitions of Dy^{3+} ions [16].Sreedhar et al., observed PL emission at 486 and 577 nm in dysprosium doped zinc fluoro phosphate glasses and they explained the emission at 486 nm due to the transition between $^4F_{9/2}$-$^6H_{15/2}$ and the emission at 577 nm due to the transition $^4F_{9/2}$ -$^6H_{13/2}$ [10]. Tyagi et al., reported a broad PL emission band ranging from 350-570 nm wavelength region with a peak around 425 nm (blue emission) for $BaWO_4$ single crystal [17].There are reports on metal tungstates showing blue luminescence due to the radiative transition within the tetrahedral group (WO_4^{2-}) [13].Thus, the obtained PL emission in the present case can be due to the radiative transitions between the sub-levels of $^4F_{9/2}$ and $^6H_{15/2}$ [17]. However in the present case yellow emission around 577 nm is not observed. The characteristics of photoluminescence of ions doped in solids depend sensitively on crystal field structure arising out of the nature of the solids [18]. Hence, spectra of same types of ions in different solid state environments will have different structures [18]. The difference in spectral features reported by Sreedhar et al., from that obtained in our present work can be due to the change in crystal field arising out of $BaWO_4$.

The mechanism of PL emission and corresponding energy levels structure can be understood from the Fig. 3(e). Theband in the 430 nm region is attributed to the lowest Stark component of the upper level ($^4F_{9/2}$) to different Stark levels of the lower levels($^6H_{15/2}$). The emissions at 412nm and 460 nm can be attributed to the transitions from the $^4F_{9/2}$ levels to the lowest and highest Stark components $^6H_{15/2}$ respectively.

In the present case B3film shows maximum intensity for PL emission and B5 film shows lowest intensity for PL emission. This is due to the conventional concentration quenching of PL emission observed in solid state solutions and doped solids. Bae et.al., reported that the surface morphology and roughness of the films had a strong response on the PL intensity [19, 20]. The films with highest rms surface roughness show enhanced PL intensity due to the possibility for strong absorption of incident light due to its increased surface area. A rough film can allow the incident light to be reflected into other portion of the film surface. This can lead to more efficient use of the excitation energy and hence superior PL intensity [20].

From the AFM analysis, it is found that the rms surface roughness is maximum (27.68 nm) for B3 film and minimum (4.17 nm) for B0 film. Thus, the highest PL intensity observed for the film B3 can be due to the high value of rms surface roughness which results in the reduction of internal reflection in films [19]. However we cannot get conclusive evidence in this aspect due to lack of sufficient data. More reasonable argument in this respect can be that arising from concentration quenching.

4. Conclusions

Nanocrystallinepure and dysprosium doped $BaWO_4$ thin films are prepared on quartz substrate by RF magnetron sputtering technique. Moderate doping of dysprosium enhances the crystalline quality of the film whereas higher dysprosium doping declines the crystalline quality. The presence of characteristic bands for the Dy^{3+}doped $BaWO_4$ films in the Ramanspectra suggests the formation of $BaWO_4$ crystalline phase in all the films. The surface morphology suggests a tendency of the smaller grains to form bigger structures with increase in dysprosium concentration. The intense bluish PL emission observed in the Dy^{3+} doped films can be attributed to transition from the lowest stark level of$^4F_{9/2}$to different stark levels of $^6H_{15/2}$. The reduction in PL intensity observed for B5 film can be due to neighbouring Dy^{3+} ions.

5. References

1. S.H.Yu, M. Antonietti, H.Colfenand J. Hartmann,:*Nano Letters,*3, 379 (2003).
2. J. Liao, H. You, S. Zhang, J. Jiang, B. Qiu, H. Huang and H. Wen,:*J. Rare Earths*, 29,623 (2011).
3. X.Wu, J. Du, H. Li, M.Zhang, B.Xi, H. Fan, Y. Zhu andY .Qian,:*J. Solid State Chem,*180,3288 (2007).
4. K. Hong, M. Xie, R. Hu and H. Wu,: Appl. Phys. Lett. 90, 173121 (2007).
5. T. Tesfamichael, M. Arita, T. Bostrom andJ. Bell,:*Thin Solid Films*, *518*(17), 4791(2010).
6. R.E. Tanner, A. Szekeres, D. Gogova and K. Gesheva,:*Appl. Surf. Sci*, 218, 163 (2003).
7. Y.B. Li, Y. Bando, D. Golberg and K. Kurashima,:*Chem. Phys. Lett*, 367, 214 (2003).
8. K. J. Lethy, D. Beena, R. Vinodkumar, V. P. MahadevanPillai, V .Ganesan, V .Sathe and D.M Phase,:*J.Appl. Phys*. A, 91, 637 (2008).
9. C.Lemire, B. B Lollman, A. A. Mohammad, E. Gillet andK.Aguir,:*Sens. Actuators* B,84, 43 (2001).
10. V.B. Sreedhar, D. Ramachari and C.K. Jayasankar,:*Physica* B, 408,158 (2013).

11. B.D. Cullity, *Elements of X-ray diffraction*,3rd edition,(New Jersey,Prentice Hall,1978)P.170
12. G.K. Williamson and W.H. Hall,:*ActaMetall*, 1,22 (1953).
13. N.VenugopalanPillai, V.P. MahadevanPillai, R. Vinodkumar, I. Navas,V.Ganesan and Peter Koshy,:*J.Alloy.Compd*, 509,2745 (2011).
14. S.M.Zawawi, R.Yahya, A. Hassan, H.N.M.EkramulMahmud and M.N.Daud,:*Chemistry Central Journal*, 7, 80 (2013).
15. R.S. Ajimsha, A.K. Das, B.N. Singh, P. Misra and L. M. Kukreja,:*Physica* E, 42, 1838 (2010).
16. X.Sun,X.Sun, X.LI,H.E. Jianand B.NshengWang,:*J. Electronic Materials*, 43, 3534 (2014).
17. M. Tyagi,Sangeeta andS.C. Sabharwal,: *J.Lumin*,128, 1528 (2008).
18. L. Li, W. Zi, G. Li, S. Lan, G. Ji, S.Gan, H. ZouandX. Xu,:*J. Solid State Chem,* 191, 1750(2012).
19. J.S. Bae, J.C. Park ,J.M. Park, B.C.Choi,J.H. seo, Y.S. Kim, S.S.Yi andJ.H.J.eong ,:*J.Applied Physics*. A, 78,877 (2004).
20. R.Sreeja Sreedharan, R.Vinodkumar, I. Navas, R. Prabhu and V.P. MahadevanPillai,:*The Minerals, Metals & Materials Society*; JOM, 68, 341(2016).